A STATISTICAL-COST APPROACH TO UNWRAPPING THE PHASE OF INSAR TIME SERIES

Andrew Hooper

Delft Institute of Earth Observation and Space Systems, Delft University of Technology, Delft, Netherlands, Email: a.j.hooper@tudelft.nl

ABSTRACT

Fully 3-D phase-unwrapping algorithms are commonly based on the central assumption that the phase difference between neighbouring sample points in any dimension is generally less than half a phase cycle (the Nyquist criteria). In the case of InSAR time series, however, signals are correlated spatially but uncorrelated over the repeat-pass time, due chiefly to changes in atmospheric delay. Here I present an alternative 3-D phase-unwrapping algorithm that treats the problem as a series of maximum a posteriori probability (MAP) estimation problems. This is achieved by generating probability density functions for the unwrapped phase difference between neighbouring points through analysis in time, and then searching for the solutions in space that maximise the total joint probability.

Key words: Phase-unwrapping; InSAR; PSI; SBAS.

1. INTRODUCTION

There are now many examples of time series InSAR techniques that seek to extract ever more information from SAR images. These techniques can be divided into those that rely on analysis of interferograms all with respect to the same master image, commonly known as persistent scatterer methods [e.g. 1, 2, 3], and those that analyse interferograms formed with respect to multiple
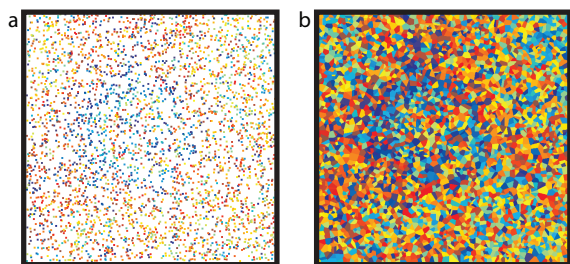

Figure 1. Interpolation in space, (a) original data points and (b) after nearest-neighbour interpolation.
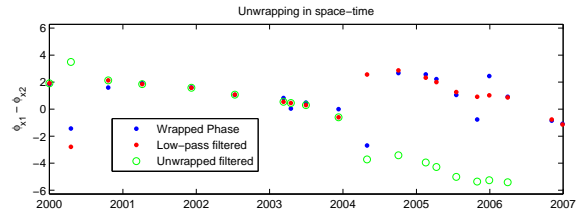

Figure 2. Filtering and unwrapping of phase-differences in time.

masters, commonly known as small baseline methods [e.g. 4, 5, 6, 7]. In both sets of algorithms, correctly estimating the integer ambiguities in the interferogram phase is a critical step. In general, the chances of success are greater when treating the entire time series as one three-dimensional (3-D) phase-unwrapping problem, rather than unwrapping the phase of each interferogram independently in 2-D [8].

Phase-unwrapping algorithms developed for 3-D data sets [e.g. 9, 10, 8] are typically based on the assumption that the phase difference between neighbouring sample points in any dimension is generally less than half a phase cycle. However, in the case of InSAR time series signals are correlated spatially, but uncorrelated over the repeat time, due to changes in atmospheric delay. This can vary by several phase cycles across an interferogram, leading to most phase differences in the time dimension being greater than half a cycle. Deformation, too, can lead to phase jumps greater than half a cycle.

On the other hand, the phase difference of a sample point with respect to a nearby sample point is likely to vary by less than half a cycle between acquisitions, because the contribution from spatially-correlated signals between points close in space is usually small. I use this fact to set up the InSAR time series phase-unwrapping problem as a series of maximum a posteriori probability (MAP) estimation problems. First, the temporal evolution of the phase difference between neighbouring samples is estimated, by unwrapping the phase difference under the assumption that it consists of a smooth deformation signal plus random noise. These estimates are used to build a probability density function for the phase dif-
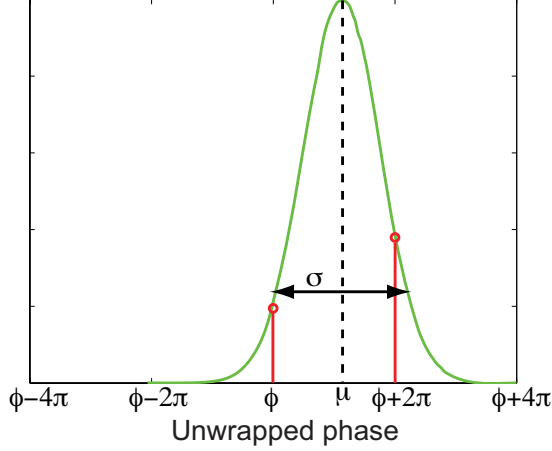
Figure 3. Unwrapped phase probability density function (PDF). The green line describes the PDF derived from estimates for the expected value of displacement, μ, and the standard deviation of the phase noise, σ. The red line gives the PDF after enforcing congruence (not scaled).

Figure 4. The time evolution of the volume of the simulated point pressure source. Red circles indicate a simulated SAR acquisition.

ference between each pair of neighbouring sample points in every interferogram.

In order to take advantage of efficient optimisation routines that exist for regularly gridded data, the phase measurements are resampled to a grid using a nearest-neighbour interpolation routine. We then apply the optimisation routines of SNAPHU [11], which uses a generalised cost function approach to find the approximate MAP solution, to each interferogram. Usually cost functions are derived within SNAPHU itself, but we set them externally such that (1) phase jumps cannot be placed between grid cells interpolated from the same sparse value and (2) the probability density function of the phase between other cells depends on the estimated evolution of the phase difference between the cells with time.

2. METHOD

To utilise efficient algorithms for spatial unwrapping developed for data sets sampled on a regular grid, e.g., SNAPHU [11], we first interpolate each sparse interferogram in the spatial domain using a nearest-neighbour algorithm (Fig. 1). This approach was first implemented in the Stanford method for persistent scatterers (StaMPS) software [12] and the validity of the method is demonstrated in [13].

The phase difference between neighbouring grid cells that were not interpolated from the same point is calculated for all interferograms. An example of the wrapped phase difference is indicated by the blue dots in Fig. 2. These wrapped phase values are low-pass filtered in time using local linear interpolation weighted by a Gaussian window. The filtered values are then unwrapped under the Nyquist assumption, i.e phase differences are inte-
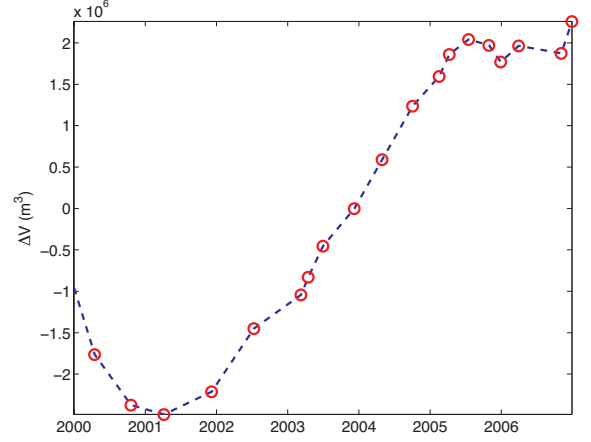
grated on the assumption that they lie between $-\pi$ and π.

The results from the filtering and phase-unwrapping in the time dimension are used to build *a priori* probability density functions (PDFs) for the unwrapped phase differences between neighbouring grid cells in each interferogram. In the case where both neighbouring cells are interpolated from the same phase measurement, the PDF is a Dirac delta function, i.e., the probability of a non-zero phase difference is zero. In all other cases, the PDF is the normalised product of a Gaussian PDF and a comb function. The maximum likelihood value of the Gaussian PDF is the temporally unwrapped, low-pass filtered value and the variance is derived from the variance of the residual between the original and low-pass filtered values (Fig. 3). The purpose of multiplying by a comb function is to enforce congruence, in other words, to ensure that the unwrapped phase can only be equal to the wrapped phase plus an integer number of cycles. The peaks are therefore at $\phi + 2n\pi$, where ϕ is the wrapped phase.

Cost functions are derived from the *a priori* PDFs by taking the negative logarithm. The optimisation routines of SNAPHU are then used to search for the minimum total cost solution for each interferogram as [14]

$$minimize\left\{-\sum_{k} log(f(\Delta\phi_k|\Delta\psi_k))\right\} \quad (1)$$

where $f(\Delta\phi|\Delta\psi)$ is the conditional probability density function of the unwrapped phase gradient between neighbouring points, conditional on the wrapped phase gradient, and the sum with index k is taken over all rows and columns. This is equivalent to maximising the total joint probability density.
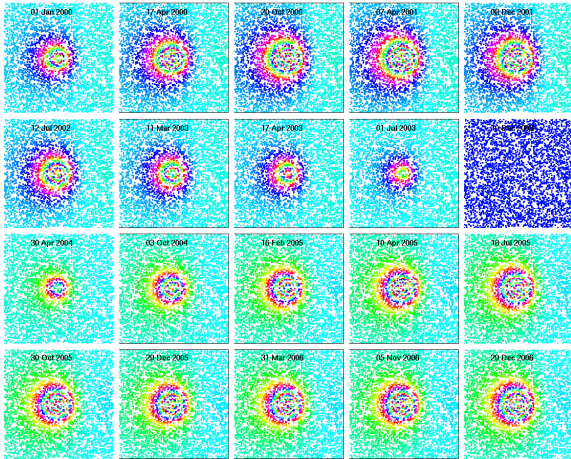
Figure 5. Wrapped phase for the line-of-sight displacement only, sampled at times given by the red circles in Fig. 4.
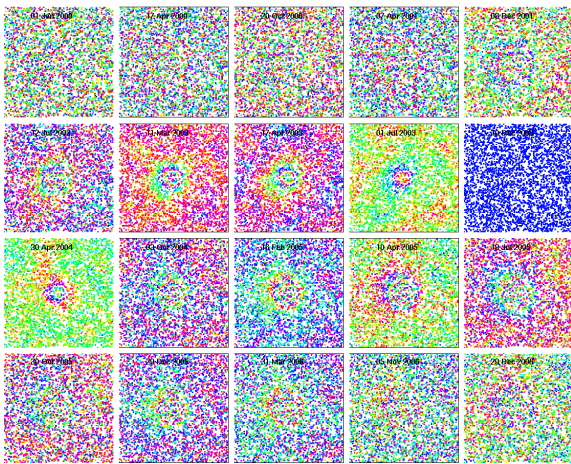

Figure 6. Simulated wrapped phase of single-master interferograms after adding atmospheric and decorrelation noise to the line-of-sight displacements shown in Fig. 5.

3. SIMULATED DATA

We generated a randomly evolving volume for a point pressure source [15] at 2 km depth (Fig 4), and simulated the line-of-sight displacements at random points for a C-band SAR with a $19°$ angle of incidence (Fig. 5). We added a realistic atmospheric phase screen to each image and decorrelation noise based on full decorrelation for a 1100 m perpendicular baseline or for 500 days between passes (Fig 6).

We unwrapped the phase of the simulated data using the new 3-D algorithm. The results (Fig. 7a) are good even when the phase seems completely decorrelated to the human eye (e.g., first few wrapped interferograms in Fig. 6), with only scattered one cycle errors (Fig. 8a). Results from 2-D unwrapping are shown for comparison in Fig. 8c.
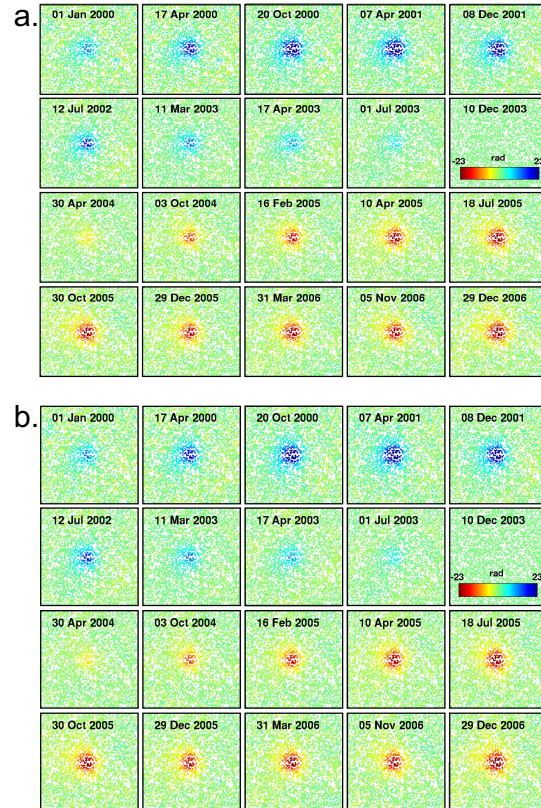

Figure 7. Unwrapped phase of interferograms. The new 3-D time series algorithm has been applied to (a) the single master time series and (b) the multiple master time series network (Fig. 9).

We also formed a network of 48 small-baseline interferograms from the original 20 images (Fig. 9) and unwrapped the phase of these interferograms. We then estimated the unwrapped phase of the interferograms with respect to a single master using weighted least-squares, with a full variance-covariance matrix estimated from the spatial coherence (Fig. 7b). Again, there are only scattered errors introduced by the phase-unwrapping, and in this case all of the errors are less than one cycle in magnitude.

4. CONCLUSIONS

We have developed an algorithm to unwrap the phase of InSAR time series that takes advantage of efficient existing algorithms. The algorithm can be applied to both single master time series of interferograms and interferograms generated from multiple master images that cover overlapping time periods. Hence it is applicable to both persistent scatterer and small baseline methods.
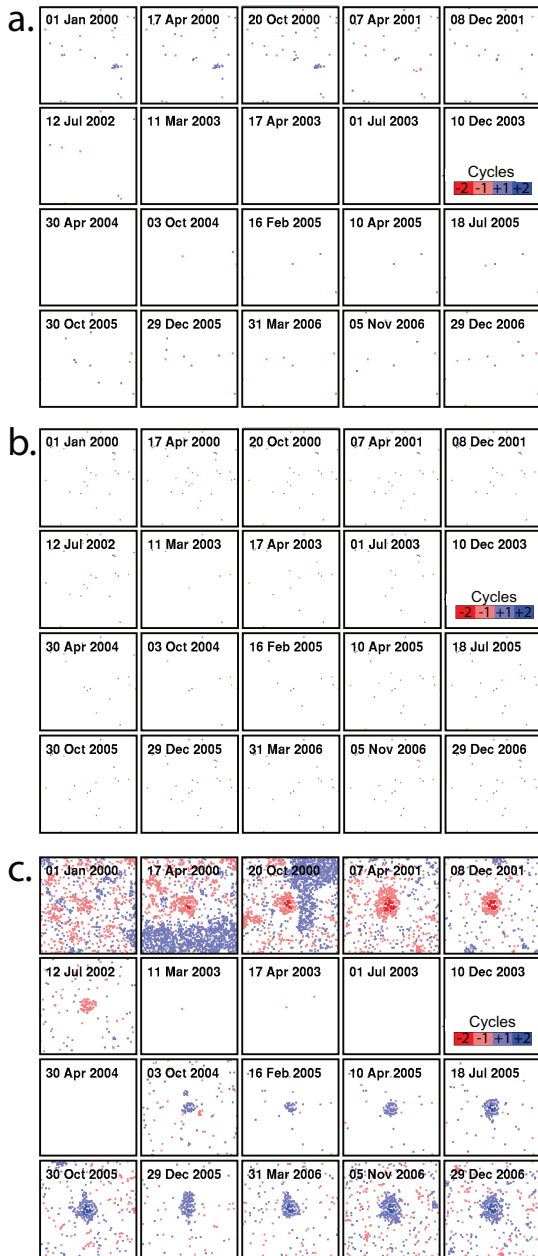
Figure 8. *Residuals between unwrapped phase and true phase using (a) the new 3-D time series algorithm applied to the single master time series, (b) the new algorithm applied to the multiple master time series network (Fig. 9) and (c) using a 2-D statistical-cost algorithm applied to the single master time series.*

Figure 9. *Small baseline network. Red circles represent acquisitions and green lines indicate the interferograms formed.*

REFERENCES

[1] A. Ferretti, C. Prati, and F. Rocca. Permanent scatterers in SAR interferometry. *IEEE Trans. Geosci. and Remote Sens.*, 39(1):8 – 20, 2001.

[2] A. Hooper, H. Zebker, P. Segall, and B. Kampes. A new method for measuring deformation on volcanoes and other natural terrains using InSAR persistent scatterers. *Geophys. Res. Lett.*, 31(23), 2004.
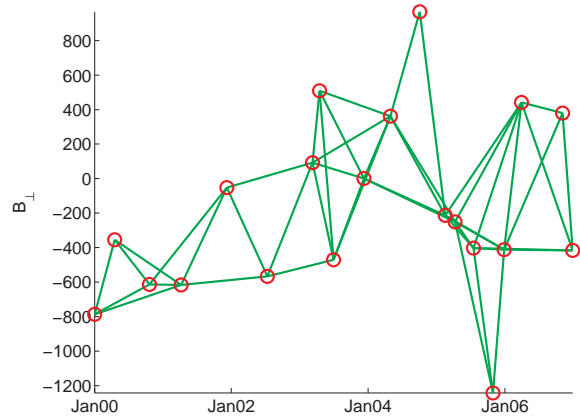
[3] B. M. Kampes. *Displacement Parameter Estimation Using Permanent Scatterer Interferometry*. PhD thesis, Delft University of Technology, 2005.

[4] P. Berardino, G. Fornaro, R. Lanari, and E. Sansosti. A new algorithm for surface deformation monitoring based on small baseline differential SAR interferograms. *IEEE Transactions on Geoscience and Remote Sensing*, 40(11):2375 – 83, 2002.

[5] D. A. Schmidt and R. Bürgmann. Time-dependent land uplift and subsidence in the Santa Clara valley, California, from a large interferometric synthetic aperture radar data set. *Journal of Geophysical Research*, 108(B9):2416 – 28, 2003.

[6] R. Lanari, O. Mora, M. Manunta, J. J. Mallorqui, P. Berardino, and E. Sansosti. A small-baseline approach for investigating deformations on full-resolution differential SAR interferograms. *IEEE Trans.Geosci. Remote. Sens.*, 42(7):1377– 1386, 2004.

[7] A. Hooper. A multi-temporal InSAR method incorporating both persistent scatterer and small baseline approaches. *Geophys. Res. Lett.*, 35:L16302, 2008.

[8] A. Hooper and H. Zebker. Phase unwrapping in three dimensions with application to InSAR time series. *J. Opt. Soc. Amer. A*, 24:2737–2747, 2007.

[9] J. M. Huntley. Three-dimensional noise-immune phase unwrapping algorithm. *Applied Optics*, 40(23):3901 – 8, 2001.

[10] M. F. Salfity, J. M. Huntley, M. J. Graves, O. Marklund, R. Cusack, and D. A. Beauregard. Extending the dynamic range of phase contrast magnetic resonance velocity imaging using advanced higher-dimensional phase unwrapping algorithms. *Journal of The Royal Society Interface*, 3(8):415– 427, 2006.

[11] C. W. Chen. *Statistical-cost network-flow approaches to two-dimensional phase unwrapping for radar interferometry*. PhD thesis, Stanford University, 2001.

[12] A. Hooper. *StaMPS (Stanford Method for Persistent Scatterers) Manual, Version 2.2*, 2007.

[13] P Agram and H Zebker. Sparse two-dimensional phase unwrapping using regular-grid methods. *IEEE Geosci. Remote Sens. Lett.*, 6(2), 2009.

[14] C. W. Chen and H. A. Zebker. Two-dimensional phase unwrapping with use of statistical models for cost functions in nonlinear optimization. *Journal of the Optical Society of America A (Optics, Image Science and Vision)*, 18(2):338 – 51, 2001.

[15] K. Mogi. Relations between the eruptions of various volcanoes and the deformations of the ground surfaces around them. *Bull. Earthquake Res. Inst. Univ. Tokyo*, 36:111 – 123, 1958.